Critical Dynamics of Vesicle Stretching Transition in Elongational Flow

Vasiliy Kantsler, Enrico Segre, and Victor Steinberg

Department of Physics of Complex Systems, Weizmann Institute of Science, Rehovot, 76100 Israel

(Received 11 February 2008; published 21 July 2008)

We present results on the stretching of single tubular vesicles in an elongation flow toward dumbbell shapes, and on their relaxation. A critical strain rate $\dot{\epsilon}_c$ exists; for strain rates $\dot{\epsilon} < \dot{\epsilon}_c$, the vesicle remains tubular but fluctuates, though its steady state extension increases with the strain rate $\dot{\epsilon}$. Above $\dot{\epsilon}_c$, first a shape transition to dumbbell occurs, and then high order shape modes become unstable, leading to a pearling state. We have quantitatively characterized the transition and found a scaling of $\dot{\epsilon}_c$ with the system parameters. A remarkable feature of vesicle tube behavior around the critical point is a slowdown of the vesicle relaxation to the final extended state in the vesicle stretching. Such feature is similar to that found in continuous phase transitions and to the critical effects recently observed for polymer molecules near the coil-stretch transition in elongation flow.

DOI: 10.1103/PhysRevLett.101.048101 PACS numbers: 87.16.D−, 87.16.dj, 82.70.Uv

Biological membranes often develop tubular structures and form dynamical tubular networks, which play a crucial role in many biological processes [1]. Giant unilamellar vesicles (GUV) have been studied as a sort of artificial proxy for biological membranes, and several techniques have been reported for inducing the formation of tubes from them, such as micropipette extraction [2], optical tweezers [3], and hydrodynamic uniform flow [4,5]. Conformational fluctuations of a vesicle membrane define its configuration entropy and therewith entropy-driven tension. The vesicle membrane in this respect behaves analogously to a linear flexible polymer molecule, whose elasticity is entropy-driven too [2]. In elongation flow, a flexible polymer molecule undergoes a conformational transformation from coiled to stretched state at a critical value of the velocity gradient (strain rate). It was recently predicted theoretically [6] and confirmed experimentally [7] that the coil-stretch transition for not very long polymer molecules is a continuous one, and is characterized by a critical slowing down of the relaxation towards the steady state conformation and by enhanced critical fluctuations. This behavior compares with the well-known critical phenomena near a thermodynamic second order (continuous) transition. Thus, the similarity in entropy-driven elasticity for both polymer molecules and membranes may lead to a similarity in their dynamics in an elongation flow. On the other hand, vesicle dynamics in elongation flow is rather unexplored. To our knowledge, the only experimental study was conducted just recently, where a wrinkling instability in time-dependent elongation flow was discovered [8]. No rheological studies of vesicle suspensions in elongation flow were ever carried out. Polymer stretching manifestly leads to marked non-Newtonian behavior, such as drastic viscosity enhancement [9]. Based on the suggested analogy, one can expect some similarity in the rheological behavior of polymer and vesicle suspensions in elongation flow as well. In this Letter, we report about the stretching of tubular shape GUVs with an initial length-to-diameter ratio $L_0/D_0 > 4.2$ by an elongation flow, from a floppy state to a dumbbell shape and further into a transient pearling state [10]. Measurements of the vesicle dynamics were conducted in the vicinity of the stagnation point ($v_x = v_y = v_z = 0$) at the middle height of a cross-slot channel of 500 μm wide and 320 μm high, via epifluorescent microscopy [11]. Experiments were performed in the range of velocity gradients $\dot{\epsilon} = 0.01$–$3\ \mathrm{s}^{-1}$. The micro channel was produced in elastomer (PDMS) by soft lithography [12]. Particle tracking velocimetry measurements of the flow field confirm that the deviation of the elongation rate $(\Delta\dot{\epsilon})_{xy}/\dot{\epsilon}$ across the size of the observation window is $<5\%$, the deviations of $\dot{\epsilon}$ in the z-direction on the scale of the vesicle are $(\Delta\dot{\epsilon})_z/\dot{\epsilon} < 5\%$, and the ratio of shear velocity gradient $\dot{\gamma}_z$ to $\dot{\epsilon}$ over the size of the vesicle does not exceed $(\Delta\dot{\epsilon})_z/\dot{\epsilon}$ [11]. GUVs were prepared by the electroformation method [13]. The lipid solutions consisted of 85% dioleoyl-phosphatidylcholine (DOPC, Sigma) and 15% fluorescent phosphatidylcholine (NBD-PC, Molecular Probes) dissolved in 9:1 v/v chloroform-methanol solvent (1.8 mg total lipids/ml), or pure DOPC in the same solvent (1.5 mg/ml) (see for details Refs. [8,14,15]).

Vesicle samples were subjected to the strong elongation flow, in order to obtain a high fraction of vesicles with large excess area. Image capturing and control of stepping motor drivers were performed by custom made Labview programs. The main limitation on the vesicle observation time due to the photo-bleaching effect of the fluorescent dye was overcome by reducing the illumination to a few strobed exposures per second with an optical chopper. This extends the observation time of an individual vesicle to up to 30 minutes, allowing to stretch and relax (by stopping the extensional flow) the same vesicle multiple times at different values of $\dot{\epsilon}$. A statistical ensemble was built by collecting data for different vesicles and various strain rates. The image sequences were analyzed by custom made routines based on the Matlab Image Processing Toolbox. The experiments were conducted at temperatures between 22 and 24 °C to keep the membrane in a liquid state.

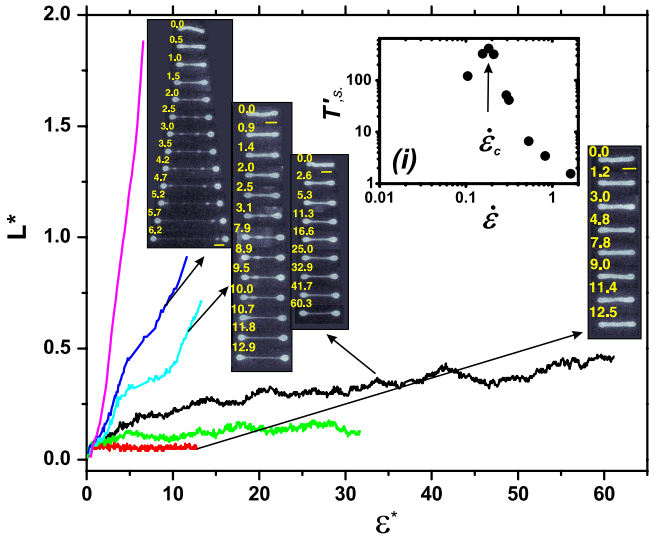

FIG. 1 (color online). Normalized vesicle extensions, $L^* = L/L_0 - 1$, as a function of the accumulated strain, ϵ^*, for six values of $\dot{\epsilon}$ in s^{-1} started from the lowest curve till the highest are shown: 0.11, 0.18, 0.21, 0.29, 0.31, 0.53. The vesicle has $L_0/D_0 = 8.8$. Time sequences of vesicle images for some values of $\dot{\epsilon}$ are also presented in the plot. Inset (i): relaxation time T' versus $\dot{\epsilon}$.

The data on the stretching of an individual vesicle, as a function of the accumulated strain, $\epsilon^* = t\dot{\epsilon}$, for different values of the elongation rate, $\dot{\epsilon}$, are shown in Fig. 1 together with the corresponding image sequences. Two factors in the experiment—the observation time of a single vesicle and the maximal extension within the field of view of a given microscope objective—limit $\epsilon^* < 60$ and the normalized tubular extension $L^* < 2$. Here, $L^* = L/L_0 - 1$, where L_0 is the initial length. For the lowest three values of $\dot{\epsilon}$ in Fig. 1, L^* saturates, while for the higher values, it apparently diverges as a function of ϵ^* in the observation frame of the vesicle extension. The transition between these two types of vesicle dynamics occurs at a critical value $\dot{\epsilon}_c$. The precise value of $\dot{\epsilon}_c$ for each vesicle with a given aspect ratio is defined by measuring the dependence of the vesicle relaxation time T' on $\dot{\epsilon}$, as explained in the following, and by locating the peak [see inset (i) in Fig. 1].

Similar relaxation dynamics was observed for vesicles with different aspect ratios L_0/D_0 from about 4.2 till 50. Regarding the elongation process, for $\dot{\epsilon} \leq \dot{\epsilon}_c$, only a slight stretching of the tubular shape vesicle is observed. At $\dot{\epsilon}_c$, tubular vesicles evolve into dumbbells. For $\dot{\epsilon} \geq \dot{\epsilon}_c$, further significant thinning and extension of the tether in the dumbbell occurs. For even higher $\dot{\epsilon}$, the tube becomes unstable, and a sequence of transitions to transient pearling configurations with different number of beads are observed. The number of beads decreases during the transient stretching, until a stationary stretched dumbbell configuration is established. Different conformation transitions with different order of unstable modes are found depending on the value of $\dot{\epsilon}$. Stretching sequences showing the pearling are presented in Fig. 2.

Figure 3 summarizes our measurements for different vesicles with different aspect ratios for 6 selected values of $\dot{\epsilon}/\dot{\epsilon}_c$. Even though the statistic is not large, particularly for higher values of $\dot{\epsilon}/\dot{\epsilon}_c$, it is sufficient to evidence the large fluctuations for $\dot{\epsilon}/\dot{\epsilon}_c = 1$. These data are obtained using different vesicles with different initial aspect ratios as well as for the same vesicle in different runs (repeated stretching after retraction). As it is presented in the plot at $\dot{\epsilon}/\dot{\epsilon}_c = 0.85$, one can find two pairs of tracks for two vesicles that show rather strong fluctuations as well as in the plot at $\dot{\epsilon}/\dot{\epsilon}_c = 1$. We did not proceed further with quantitative characterization of the apparent enhanced fluctuations to establish their source. It definitely requires separate investigation based on large vesicle statistics that will face experimental difficulties particularly due to severe limitations to observe a single vesicle for a long time. For $\dot{\epsilon}/\dot{\epsilon}_c \leq 1$, the higher the strain rate, the longer the time to reach the steady state with maximum vesicle extension, L_m^*. In order to get a quantitative dependence on $\dot{\epsilon}$ of the relaxation time T' of a single vesicle to its steady state, each individual relaxation trace, similar to the ones shown in Fig. 1, was either fitted by $L^*(t) \sim 1 - \exp(-t/T')$ for $\dot{\epsilon}/\dot{\epsilon}_c \leq 1$, or by $T' = [\frac{\Delta L^*}{\Delta t}]^{-1}$ for $\dot{\epsilon}/\dot{\epsilon}_c > 1$. The normalized and averaged form, for all vesicles, of the dependence of $T = \langle T' \rangle$ on the scaled elongation rate, $\dot{\epsilon}/\dot{\epsilon}_c$, was obtained from either the averaged fits of the scaled individual dependencies $T'(\dot{\epsilon}/\dot{\epsilon}_c)$ or from the fits of the ensemble average traces in Fig. 3, and is presented in the inset in Fig. 4. Significant increase in the vesicle relaxation time at the conformation transition from the tubule-to-dumbbell

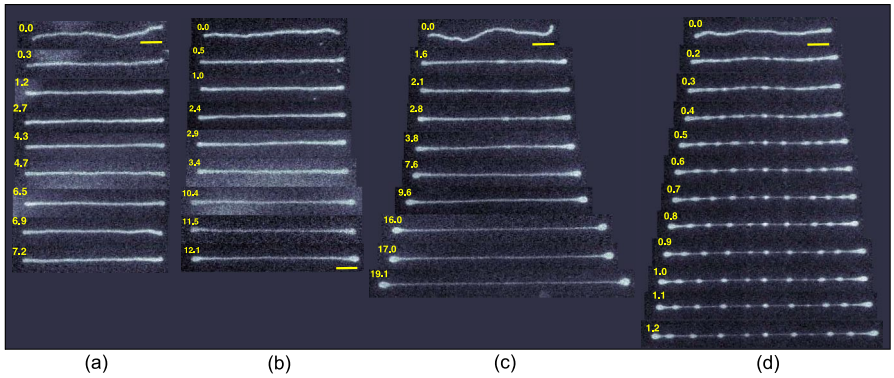

FIG. 2 (color online). Stretching of a tubular vesicle. Parameters of the tube are $L_0 = 66\ \mu$m, $D_0 = 1.4\ \mu$m, $L_0/D_0 \simeq 47$, $\eta = 5.4 \cdot 10^{-3}$ Pas. (a) $\dot{\epsilon} = 0.09\ s^{-1}$. (b) $\dot{\epsilon} = 0.14\ s^{-1}$ (dumbbell mode instability). (c) $\dot{\epsilon} = 0.19\ s^{-1}$ (second mode instability—pearling). (d) $\dot{\epsilon} = 0.92\ s^{-1}$. Scale bar is $10\ \mu$m, numbers are ϵ^*.

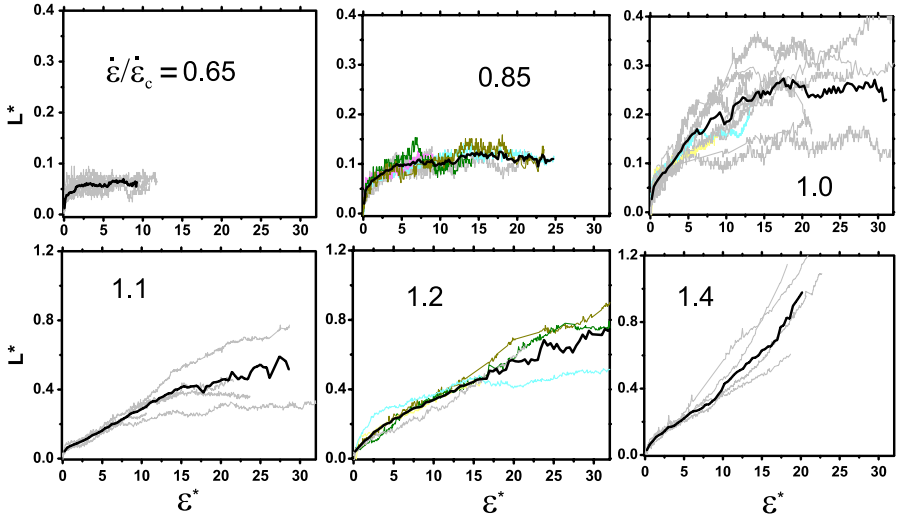

FIG. 3 (color online). Individual and ensemble average normalized vesicle extension versus ϵ^* for 6 values of $\dot{\epsilon}/\dot{\epsilon}_c$. All the gray tracks represent different vesicles, black is the average. $\dot{\epsilon}/\dot{\epsilon}_c = 0.65$–8 tracks. $\dot{\epsilon}/\dot{\epsilon}_c = 0.85$–8 tracks, 4 highlighted tracks are for the vesicle $L_0 = 33.8\ \mu$m, $D_0 = 1.8\ \mu$m, and the vesicle $L_0 = 29.3\ \mu$m, $D_0 = 2.5\ \mu$m. $\dot{\epsilon}/\dot{\epsilon}_c = 1$–11 tracks, 2 highlighted tracks are for the vesicle $L_0 = 54.5\ \mu$m, $D_0 = 1.7\ \mu$m. $\dot{\epsilon}/\dot{\epsilon}_c = 1.1$–5 tracks. $\dot{\epsilon}/\dot{\epsilon}_c = 1.2$–6 tracks, 4 highlighted tracks are for the vesicle $L_0 = 32\ \mu$m, $D_0 = 1.9\ \mu$m, and for the vesicle $L_0 = 33.8\ \mu$m, $D_0 = 1.8\ \mu$m. $\dot{\epsilon}/\dot{\epsilon}_c = 1.4$–4 tracks.

shape, which indicates the critical slowdown, is noticeable. We found also that the critical $\dot{\epsilon}_c$ for the transition first to dumbbell and further transition to pearling strongly depend on L_0/D_0 (see Fig. 4). To collapse the data, the values of $\dot{\epsilon}_c$ are scaled, in the main plot, by the characteristic retraction time of the vesicle to its equilibrium state, after flow cessation. This characteristic time τ is defined below from a simple model, though it could be found also experimentally (see inset in Fig. 5). We could not observe vesicle stretching for $L_0/D_0 < 4.2$, since $\dot{\epsilon}_c$ diverges at small L_0/D_0, as seen from Fig. 4. Because of this aspect ratio dependence, the traces of different vesicles with different aspect ratios can be presented on a single plot in Fig. 3 only after rescaling $\dot{\epsilon}$ with $\dot{\epsilon}_c(L_0/D_0)$.

In order to characterize quantitatively the recover of the tubular vesicle to its rest state, we measure the relaxation (retraction) time of each vesicle by first stretching it with the elongation flow and then ceasing the flow, as was done for polymer molecules [16,17]. In the inset in Fig. 5, we show the data for one individual vesicle recoil together with its exponential fit. Such exponential decay is observed if the elongation rate does not exceed the critical value for the onset of the tube pearling instability. Finally, the steady state vesicle extension, L_m^*, grows continuously as a function of $\dot{\epsilon}/\dot{\epsilon}_c$ through the conformation transition onset as shown in Fig. 5.

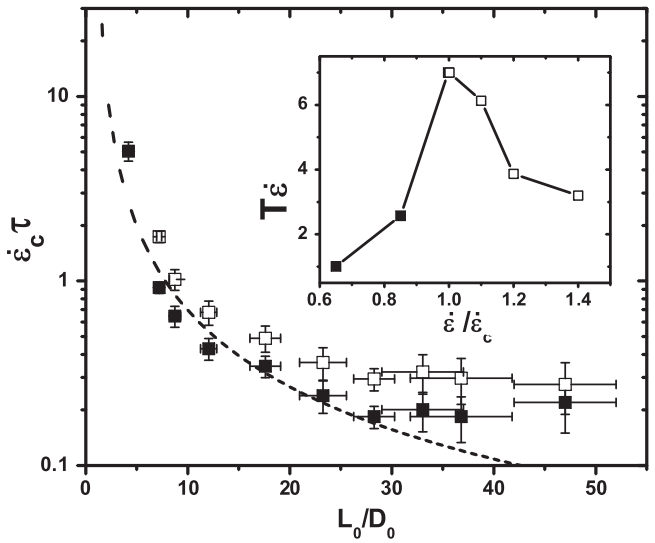

FIG. 4. Normalized critical elongation rate, $\dot{\epsilon}_c\tau$, versus L_0/D_0 for both tubular-dumbbell transition (full squares) and tube instability to pearling state (open squares). The dashed line is $\dot{\epsilon}_c\tau \sim (D_0/L_0)\ln(L_0/D_0)$. Inset: Normalized relaxation time of all vesicles, $\dot{\epsilon}T$, versus $\dot{\epsilon}/\dot{\epsilon}_c$. Full squares are for data obtained from ensemble averaging of individual T' from the exponential fits, while the open squares are defined from ensemble averaging of the initial slope of relaxation curves (see Fig. 3).

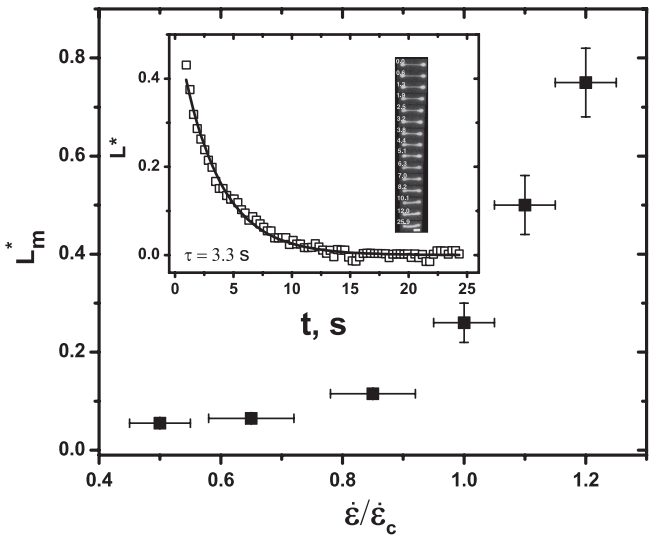

FIG. 5. Ensemble averaged maximum vesicle extension, L_m^*, versus $\dot{\epsilon}/\dot{\epsilon}_c$ (up to tube instability threshold). Inset: $L^*(t)$ during the retraction of an individual vesicle to the rest state, together with the exponential fit. The time sequence of images during relaxation is also shown.

To estimate the vesicle retraction time from the dumbbell to the rest configuration, let us consider a dumbbell object like that attained by a vesicle stretched above the stretching transition. It can be modeled by two spheres of radius R and a tether of length L and radius r. As the largest part of the vesicle volume is contained in the spheres and almost does not change, R remains unchanged during stretching, due to volume conservation. At the same time, most of the membrane surface area $S \sim rL$, which remains constant too, is accounted for by the tether. Each sphere is pulled back by the entropic force of the vesicle membrane, $f_e \sim r\sigma \sim \kappa/r \sim \kappa L/S$. Here, σ is the surface tension, and κ is the membrane bending elasticity, which for DOPC is measured as $\kappa = 10^{-12}$ erg [18]. This force balances the Stokes drag on the moving spheres, $f_{\mathrm{St}} \sim \eta R\dot{L}$. The balance gives then the equation for the vesicle retraction $-\dot{L}/L \sim \kappa/(RS\eta)$, whose solution is the exponential decay observed experimentally (see inset in Fig. 5): $L \sim \exp(-t/\tau)$, where $\tau \sim RS\eta/\kappa$ is the vesicle relaxation (retraction) time.

The critical elongation rate for the dumbbell transition can be estimated by a similar argument. Let us consider a tubular shape vesicle before the transition, having length L_0 and diameter D_0, placed in an extensional flow with strain rate $\dot{\epsilon}$. The stretching Stokes force along the cylinder $f_{\mathrm{St}} \sim L_0^2\dot{\epsilon}\eta/\ln(L_0/D_0)$ is balanced by the entropic force $f_e \sim D_0\sigma \sim \kappa L_0/S$, where $S \sim D_0L_0$. Transition occurs when the hydrodynamical drag force exceeds the entropical tension of the tube, i.e., for $\dot{\epsilon}_c\tau \sim (D_0/L_0)\ln(L_0/D_0)$. The inverse dependence of the normalized critical elongation rate, $\dot{\epsilon}_c\tau$, on the vesicle aspect ratio, L_0/D_0, agrees well with the experimental observation (see Fig. 4), where $\tau = D_0^2L_0\eta/4\kappa$.

To summarize, we found and investigated the sequence of conformational transitions underwent by a tubular vesicle stretched by an elongation flow. First, we quantitatively analyzed the transition from the tubule to the dumbbell vesicle configuration, which is accompanied by the slowing down of the dynamics of the vesicle extension near the threshold value of the elongation rate, $\dot{\epsilon}_c$. We guess that the observed slowing down occurs due to presence of a large number of possible vesicle configurations available close to the transition point, when the entropic force (elasticity) is balanced by the hydrodynamic drag (stretching force). This critical effect is a characteristic feature and unique signature of the stretching transition and show, strikingly, how a simple elongation flow has a nontrivial influence on the dynamics of a single vesicle. We furthermore observe that vesicle stretching is strongly nonaffine since, for example, at an accumulated strain of $\epsilon^* = 30$, the stretching of a passive fluid element at the location of the vesicle is already many orders of magnitude larger than the extension attained by the vesicle.

The remarkable critical feature of the stretching transition is similar to those, well known, seen in continuous thermodynamic phase transitions. Thus, we suggest that the critical effect is a universal dynamical phenomenon, which occurs in any microscopic and mesoscopic objects, where thermal noise leads to large variety of accessible configurations close to the conformation transition. At $\dot{\epsilon} > \dot{\epsilon}_c$, higher order modes become unstable, leading to the further different conformation transitions with different numbers of unstable modes. The latter results in the previously observed transient pearling states with different number of beads [10].

We thank V. Lebedev for helpful remarks and illuminating discussions. We thank the referees for the useful and constructive remarks and criticism. This work is partially supported by the grants of the Israel Science Foundation, the Minerva Foundation, the Israeli Ministry of Science, Culture & Sport for Russian-Israeli Cooperation, and by the Minerva Center for Nonlinear Physics of Complex Systems.

[1] C. Lee and L. B. Chen, Cell **54**, 37 (1988); H. Mollenhauer and D. Morre, Histochem. Cell Biol. **109**, 533 (1998); R. Bar-Ziv *et al.*, Proc. Natl. Acad. Sci. U.S.A. **96**, 10140 (1999); P. Pulalrkat *et al.*, Phys. Rev. Lett. **96**, 048104 (2006).
[2] E. Evans and W. Rawicz, Phys. Rev. Lett. **64**, 2094 (1990); J.-B. Fournier, A. Ajdari, and L. Peliti, Phys. Rev. Lett. **86**, 4970 (2001).
[3] J. Dai and M. Sheetz, Biophys. J. **77**, 3363 (1999).
[4] O. Rossier *et al.*, Langmuir **19**, 575 (2003).
[5] N. Borghi, O. Rossier, and F. Brochard-Wyart, Europhys. Lett. **64**, 837 (2003).
[6] D. Vincenzi and E. Bodenschatz, J. Phys. A **39**, 10691 (2006); A. Celani, A. Puliafito, and D. Vincenzi, Phys. Rev. Lett. **97**, 118301 (2006).
[7] S. Gerashchenko and V. Steinberg, Phys. Rev. Lett. (to be published).
[8] V. Kantsler, E. Segre, and V. Steinberg, Phys. Rev. Lett. **99**, 178102 (2007).
[9] R. Bird, C. Curtiss, R. Armstrong, and O. Hassager, *Dynamics of Polymeric Liquids* (John Wiley, New York, 1987).
[10] R. Bar-Ziv and E. Moses, Phys. Rev. Lett. **73**, 1392 (1994).
[11] See EPAPS Document No. E-PRLTAO-101-075829 for schematic of experimental setup and results of velocity field measurements. For more information on EPAPS, see http://www.aip.org/pubservs/epaps.html.
[12] Y. N. Xia and G. M. Whitesides, Annu. Rev. Mater. Sci. **28**, 153 (1998).
[13] M. I. Angelova, S. Soleau, P. Meleard, J.-F. Faucon, and P. Bothorel, Prog. Colloid Polym. Sci. **89**, 127 (1992).
[14] V. Kantsler and V. Steinberg, Phys. Rev. Lett. **95**, 258101 (2005); V. Kantsler and V. Steinberg, Phys. Rev. Lett. **96**, 036001 (2006).
[15] V. Kantsler, E. Segre, and V. Steinberg, Europhys. Lett. (to be published).
[16] T. Perkins, D. Smith, and S. Chu, Science **276**, 2016 (1997).
[17] S. Gerashchenko, C. Chevallard, and V. Steinberg, Europhys. Lett. **71**, 221 (2005).
[18] W. Rawicz *et al.*, Biophys. J. **79**, 328 (2000).